Science of the Total Environment 773 (2021) 145589

Contents lists available at ScienceDirect

Science of the Total Environment

journal homepage: www.elsevier.com/locate/scitotenv

# Spatial extent of road pollution: A national analysis

Benjamin B. Phillips [a,*], James M. Bullock [b], Juliet L. Osborne [a], Kevin J. Gaston [a]

[a] *Environment and Sustainability Institute, University of Exeter, Penryn Campus, Penryn, Cornwall TR10 9FE, UK*
[b] *UK Centre for Ecology and Hydrology, Maclean Building, Wallingford, Oxfordshire OX10 8BB, UK*

## HIGHLIGHTS

- Roads form vast, pervasive and growing networks with diverse environmental impacts.
- We modelled the spatial distribution of road pollution across Great Britain.
- Half of land in Great Britain is less than 216 m from a road.
- Roads have a zone of influence that extends across >70% of the land area.
- High road pollution levels are relatively localised, but low levels are pervasive.

## GRAPHICAL ABSTRACT

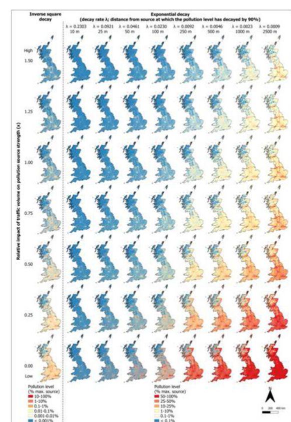

## ARTICLE INFO

*Article history:*
Received 30 November 2020
Received in revised form 28 January 2021
Accepted 29 January 2021
Available online 6 February 2021

Editor: Philip K. Hopke

*Keywords:*
Highways
Road-effect zone
Pollution
Noise
Light
Metals
Air pollution
Particulate matter

## ABSTRACT

Roads form vast, pervasive and growing networks across the Earth, causing negative environmental impacts that spill out into a 'road-effect zone'. Previous research has estimated the regional and global extent of these zones using arbitrary distances, ignoring the spatial distribution and distance-dependent attenuation of different forms of road environmental impact. With Great Britain as a study area, we used mapping of roads and realistic estimates of how pollution levels decay with distance to project the spatial distribution of road pollution.

We found that 25% of land was less than 79 m from a road, 50% of land was less than 216 m and 75% of land was less than 527 m. Roadless areas were scarce, and confined almost exclusively to the uplands (mean elevation 391 m), with only ca 12% of land in Great Britain more than 1 km from roads and <4% of land more than 2.5 km from roads. Using light, noise, heavy metals, $NO_2$, and particulate matter $PM_{2.5}$ and $PM_{10}$ as examples, we estimate that roads have a zone of influence that extends across >70% of the land area. Potentially less than 6% of land escapes any impact, resulting in nearly ubiquitously elevated pollution levels. Generalising from this, we find that, whilst the greatest levels of road pollution are relatively localised around the busiest roads, low levels of road pollution (which may be ecologically significant) are pervasive.

Our findings demonstrate the importance of incorporating greater realism into road-effect zones and considering the ubiquity of road pollution in global environmental issues. We used Great Britain as a study area, but the findings likely apply to other densely populated regions at present, and to many additional regions in the future due to the predicted rapid expansion of the global road network.



* Corresponding author.
*E-mail address:* B.B.Phillips@exeter.ac.uk (B.B. Phillips).

https://doi.org/10.1016/j.scitotenv.2021.145589
0048-9697/

## 1. Introduction

Roads form vast and pervasive networks across the Earth, with an overall estimated length of 64 million km (van der Ree et al., 2015). The associated pollution and other negative environmental impacts spill out even further, forming a ‘road-effect zone’. Understanding the extent of these impacts is critical for identifying where environmental protections (e.g. from further road building), environmental mitigations (e.g. pollution reduction) and environmental enhancements (e.g. habitat creation) will most benefit the health of both people and nature. It can also provide insights into how the environmental impacts of roads will be affected by future changes in road use (e.g. road growth and increasing traffic volumes) and associated technologies (e.g. uptake of ultra-low emission vehicles).

Previous attempts to understand the impacts of roads on the environment over large regions have generally related road proximity to specific environmental impacts, often using single thresholds for the extent of the road-effect zone (e.g. 1 km) (Forman, 2000; Ibisch et al., 2016; Psaralexi et al., 2017; Torres et al., 2016). Such approaches have estimated that 20% of land suffers environmental impacts of roads (though the underlying global road maps are very incomplete for some regions) (Hughes, 2017; Ibisch et al., 2016). Whilst there is a strong environmental case for preserving roadless areas (often defined as areas more than 1 km from any road; Ibisch et al., 2016; Psaralexi et al., 2017; Selva et al., 2011), many regions have few such areas remaining (e.g. central and western Europe; Psaralexi et al., 2017), and roads provide important social and economic benefits that motivate further road building (Laurance et al., 2014). Indeed, roadless areas will likely become increasingly scarce, given that the global road network is predicted to expand by a further 25 million paved road lane-kilometres (a 65% increase) by 2050 (Dulac, 2013). As a result, there is a need to go beyond identifying ‘where is’ versus ‘where is not’ affected by roads, and towards understanding how the intensity of environmental impacts of roads varies across space, in terms of different types of impact.

In reality, the intensity of road impacts shows spatial complexity, decreasing with distance from the road and often increasing with traffic volume. Furthermore, the environmental impact of roads is the result of diverse forms of pollution, including light, noise, vibration, de-icing salt, metals, herbicides, and exhaust emissions (e.g. $NO_x$, CO and particulates), alongside other effects (e.g. habitat fragmentation and vehicle-wildlife collisions) (Forman et al., 2003). Of these, noise and air pollution have received by far the most attention due to their impacts on human health, for which they are considered to be the most prevalent environmental risk factors in Europe (Hänninen et al., 2014). Roads are a major contributor to both. In fact, the World Health Organization (2011) states that “sleep disturbance and annoyance, mostly related to road traffic noise, comprise the main burden of environmental noise”. However, whilst air pollution is regulated in many countries, with strict limits on roadside pollution and emissions from individual vehicles (European Commission, 2021a, 2021b), noise pollution is scarcely regulated or enforced. Whilst recommended limits exist (World Health Organization, 2018), these guidelines are rarely backed up by legislation. For example, in the UK there are noise limits for individual vehicles, but no legal limits for road noise overall (UK Government, 2021). Furthermore, the diverse other forms of road pollution are almost completely ignored by policy.

Different forms of road pollution vary in their spatial distributions with respect to roads, in particular how they attenuate over distance. Many pollutants are deposited near to roads, for example metals arising from vehicles and road surfaces are principally found in soils within 15 m of roads (Werkenthin et al., 2014). Other pollutants are more far reaching, with many air pollutants found at elevated levels at distances of hundreds of meters from roads (Karner et al., 2010). Whilst dispersion patterns are highly variable among pollutants, in the broadest sense the way that a pollutant attenuates over distance depends on whether it consists of energy waves (e.g. light and noise) or matter (e.g. metals and air pollutants). Specifically, particle pollution such as metals and air pollutants are largely transported via diffusion, whereas light and noise are energy waves travelling via vibrations. Their patterns of dispersal over distance therefore differ, and in general, can be described, respectively, by exponential decay and inverse square decay functions (Attenborough, 2014; Karner et al., 2010).

Whilst numerous models of road pollution exist, they focus on individual forms of pollution, covering a limited subset of pollutants – primarily air pollutants (Tsagatakis et al., 2019) and noise (Extrium, 2020). They are usually limited to a local scale (meters to kilometres rather than hundreds of kilometres) in urban areas, and are often complex, requiring extensive data sources, parameter estimates and computational power (e.g. see Bendtsen, 1999; Forehead and Huynh, 2018; Khan et al., 2018; Murphy et al., 2020; Pinto et al., 2020; Silveira et al., 2019). Or, otherwise, they model only the largest road types (Extrium, 2020) and ignore the potential contribution of smaller roads. Here, using Great Britain as a study area and considering diverse forms of pollution, we determine the spatial distribution of road pollution, with respect to distance from roads and types of road. The study aims to: 1. Provide a more complete understanding of the road-effect zone by considering diverse forms of pollution; and 2. Provide a national-scale assessment as a case study for determining the proximity of land to roads and the proportion of land affected by different threshold levels of pollution. The findings are important for understanding the extent and degree of roads' influences on the environment, with implications for both human and ecosystem health.

## 2. Methods

We used spatial mapping and analyses in QGIS 3.4.15 (QGIS Development Team, 2020) to determine the distribution of road pollution across Great Britain. The process involved the following steps, described in detail below and summarised here: (i) categorising roads into four types based on their traffic volumes and mapping the distance of every 1 ha square of land in GB to roads of each type; (ii) creating general models of the spatial distribution of different forms of road pollution based on the following parameters: pollution source strength across road types, background pollution level, and pollution dispersion pattern with distance from the road; (iii) conducting a literature search to determine known parameter values for different forms of road pollution (metals (Cd, Cr, Cu, Ni, Pb, and Zn), air pollutants ($NO_2$, $PM_{2.5}$ and $PM_{10}$), light and noise); (iv) modelling spatial distributions for these forms of road pollution by parameterising the models from (ii) with values from (i) and (iii); and (v) generalising our findings, given limitations on available data for real forms of road pollution, by modelling spatial distributions of theoretical pollution groups that differ in the outlined parameters, across a range that encompasses those of real forms of road pollution.

### 2.1. Spatial maps of road proximity

To map roads, we used freely available data from OS OpenData (Ordnance Survey, 2020): OS Open Roads and OS Boundary-Line. OS Open Roads is a vector map of all roads in Great Britain, including information on road classification. OS Boundary-Line contains vectors of Great Britain and its administrative boundaries. We merged component layers of OS Open Roads into a single shapefile and removed duplicated sections of road. We aggregated roads into four types (which we will term $r$) based on road classification (from OS Open Roads) and the availability of associated traffic volumes (from UK Government data; Department for Transport, 2019) (Table 1). These types were (in order of highest to lowest traffic volume) motorways, A-roads, minor roads, and local access roads.

We created a grid of points with 100 m intervals across the extent of Great Britain, then clipped the grid using a polygonised high-water

**Table 1**
The road types *r* that were used for the spatial mapping and analyses of road pollution. Maps of the proximity to roads of each road type are provided in Fig. 1b–e.

| Road type *r* | OS Open Roads road class(es) | OS Open Roads road length (km) | UK Government road length (km)[a] | Proportion of total road length | UK Government traffic volume (vehicles $day^{-1}$)[b] | Relative traffic volume |
|---|---|---|---|---|---|---|
| Motorways ($r = 1$) | Motorways | 5141 | 3742 | 0.0074 | 81,700 | 1.0000 |
| A-roads ($r = 2$) | A-roads | 49,659 | 47,450 | 0.0719 | 13,800 | 0.1689 |
| Minor roads ($r = 3$) | B/Minor/Local roads | 341,684 | 346,405 | 0.4947 | 1400 | 0.0171 |
| Local access roads ($r = 4$) | Local Access/ Restricted Local Access/Secondary Access roads | 294,196 | Not provided | 0.4260 | Not available, so assumed 70 (5% of minor roads) | 0.0009 |

[a] Department for Transport (2020). Road lengths statistics (RDL). Data for 2019. https://www.gov.uk/government/statistical-data-sets/road-length-statistics-rdl.
[b] Department for Transport (2019). Road traffic statistics (TRA) statistical data set. Data for 2018. https://www.gov.uk/government/statistical-data-sets/road-traffic-statistics-tra.

polyline shapefile from OS Boundary-Line. We calculated the distance to the centreline of the nearest road for each grid point, then converted this information to a raster with 100 m resolution, resulting in the value of each cell representing the distance to the nearest road of the centroid of the cell (Fig. 1a). We repeated this process for each of the four road types, resulting in a 100 m raster of distances to the nearest road for each road type (Fig. 1b–e). As the distance to the nearest road used a centreline for each road, we accounted for differences in road widths between road types by assuming that: (i) pollution originates from the centre of the outermost lanes of a road, (ii) road lanes are 3.65 m wide (Department for Transport, 2020a) and (iii) the number of lanes per direction is 3 for motorways, 1.5 (1 to 2) for A-roads, 0.75 (0.5 to 1) for minor roads and 0.625 (0.5 to 0.75) for local access roads. We therefore subtracted the following distances from all cells (bounded above zero) of the respective road type raster: 9.125 m for motorways (Fig. 1b), 4.5625 m for A-roads (Fig. 1c), 1.3688 m for minor roads (Fig. 1d) and 1.1406 m for local access roads (Fig. 1e).

For context, we estimated the area of land covered by roads by multiplying the width of a road lane (3.65 m wide; Department for Transport, 2020a) by the estimated number of lanes per road of each road type (see above), then multiplying by the length of road of each type (from UK Government data for 2019; Department for Transport, 2020; see Table 1). We also assessed the land cover and elevation of roadless areas (>1 km from roads) using CORINE Land Cover (Copernicus, 2018) and OS Terrain 50 (Ordnance Survey, 2020).

### 2.2. General modelling approach

We built two general models of the spatial distribution of road pollution: one for pollution caused by energy waves (such as light and noise) and one for pollution consisting of matter (such as metals, particulate matter and $NO_2$). These models were later parameterised from the literature for different types of pollution. The modelling approach was based on differences in (i) pollution source strength *a* (the pollution level at a road) across road types *r* (the four road types described above, differing in traffic volume), (ii) background pollution level *b* (the pollution level in the absence of roads), and (iii) dispersion patterns (the function by which pollution disperses from a road, consisting of decay type – inverse square or exponential – and, in the latter case, decay rate λ). We modelled levels of pollution exclusively attributable to roads by subtracting the background pollution level *b* from the pollution source strength *a*, which meant that modelled road pollution levels attenuated to zero, rather than to the background level. In reality, there are many other sources of pollutants, which combine to result in overall pollution levels; but in this case, pollution arising specifically from roads was of principal interest.

Given the large number of complex variables involved in modelling just a single pollutant (e.g. see Khan et al., 2018; Pinto et al., 2020), it was necessary to make assumptions and simplifications, which we describe throughout. In general though, we used average values across space and time, whereas traffic volumes differ between urban and rural areas, among geographic regions, and across the time of day and week (Department for Transport, 2019), and dispersion of pollutants is affected by meteorological conditions, which can also result in strong asymmetry between opposite sides of a road (Forman et al., 2003). We did not incorporate pollution mitigation by vegetation, terrain and other barriers, so our estimates are rather representative of maximum potential extent. We address the implications of these assumptions in the discussion.

#### 2.2.1. Pollution source strength

We assumed that differences in pollution source strengths among road types were related to traffic volumes. This is because most road pollutants arise either directly from vehicles (e.g. noise and exhaust emissions), or indirectly from roads themselves (e.g. particles from wear of road surfaces) and their management (e.g. de-icing salt), whereby roads with greater traffic volume are likely to be larger and receive more intensive management (Forman et al., 2003). However, the strength of the relationship between pollution source strength and traffic volume likely varies among pollutants and may have a weak relationship (e.g. heat originating from the road surface, light originating from street lighting) or possibly no relationship. As such, we calculated relative pollution source strengths for each road type based on the relative impact of traffic volume on the pollution source strength. We used the following equation:

$$a_r = (t_r/t_1)^x \quad (1)$$

where $a_r$ is the pollution source strength for road type *r*, $t_r$ is the average daily traffic volume for road type *r* (from UK Government data for 2018; Department for Transport, 2019; Table 1), $t_1$ is the average daily traffic volume for the highest traffic volume road type (motorways) and *x* is a scaling variable defining the relative impact of traffic volume on the pollution source strength.

#### 2.2.2. Decay rates

We modelled the attenuation of pollution strength from a point source over an uninterrupted linear distance from a road using two different decay functions, which are well established for different forms of pollution. For simplicity, these equations represent the decay from a point source, representing the straight-line distance to the nearest road. 1. Inverse square decay, to represent pollution types that consist of energy waves (e.g. light and noise; Attenborough, 2014):

$$p_e = (a-b)d^{-2} \quad (2)$$

where *p* is the pollution level, *a* is the pollution source strength, *b* is the background pollution level, and *d* is the distance to the nearest road. 2.

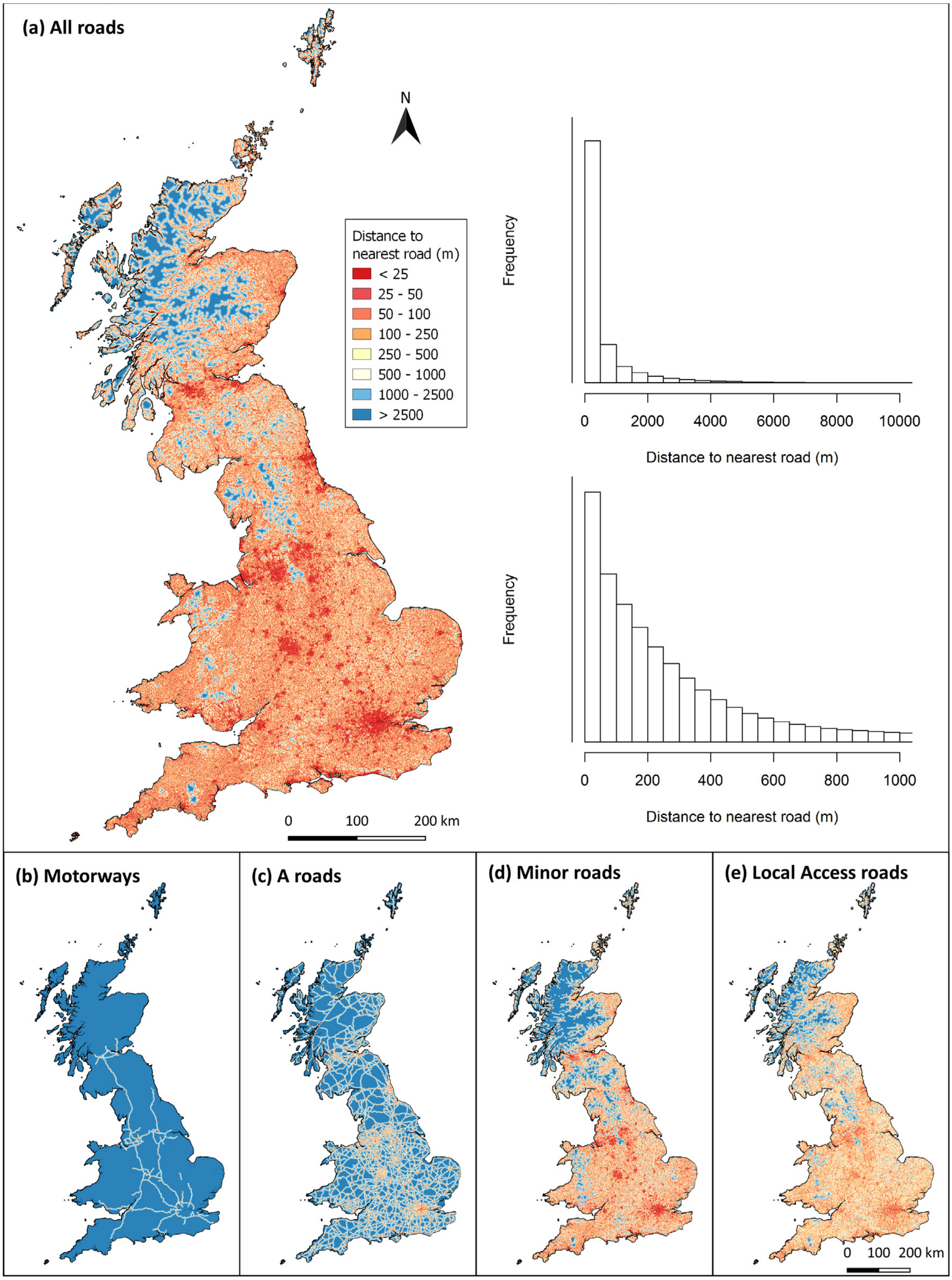


**Fig. 1.** Distances to the nearest road from the centre of each 1 ha (0.01 km$^2$) area across Great Britain for (a) all roads, and associated frequency histogram (on two different scales for clarity of presentation), and (b–e) the four component road types that were used as input parameters for spatial models and analyses of road pollution.

Exponential decay to represent pollution types that consist of matter (e.g. particulates; Karner et al., 2010):

$$p_m = (a - b)e^{-\lambda d} \quad (3)$$

where λ is the decay rate.

*2.2.3. Spatial modelling*

Using Eqs. (2) and (3), we modelled the pollution level in each 100 m grid cell attributable to the nearest road of each road type as:

$$p_{e_r}(d_r) = (a_r - b)d_r^{-2} \quad (4)$$

for pollution types that consist of energy waves, and

$$p_{m_r}(d_r) = (a_r - b)e^{-\lambda d_r} \quad (5)$$

for pollution types that consist of matter, where $a_r$ is the pollution source strength for road type $r$, and $d_r$ is the distance to the nearest road of road type $r$ (from Fig. 1). We calculated the total pollution level in each grid cell by adding together the pollution level attributable to each of the four road types, resulting in the final equations:

$$p_{e_{total}} = \sum_{r=1}^{4} p_{e_r}(d_r) \quad (6)$$

for pollution types that consist of energy waves, and

$$p_{m_{total}} = \sum_{r=1}^{4} p_{m_r}(d_r) \quad (7)$$

for pollution types that consist of matter. This assumes that pollution from multiple roads of different types is additive, but ignores additional nearby roads of the same type (e.g. in urban areas where numerous minor roads are located within a small area, resulting in overlapping, additive accumulation of pollution, such as around junctions). It also assumes that the pollution level in a cell is not affected directly by the pollution level in neighbouring cells.

### *2.3. Literature search for parameter values*

We conducted a literature search to find parameter values for different forms of road pollution. We searched Web of Science Core Collection databases (in English language only) for scientific publications published up to January 2020. We limited the search to reviews and meta-analyses due to an abundance of literature on the topic, and only to those which focused on Europe and/or North America to ensure relevance to Great Britain (in terms of road and vehicle technologies and usage). We used a 'road pollution' search string and combined it with a 'dispersion' search string (Table A). We assessed the relevance of each search result using the title and abstract (or full text where necessary). Of 471 search results, we identified five relevant studies, which provided information on the spatial distributions, with respect to roads, of metals in soils (Werkenthin et al., 2014), air pollutants (DeWinter et al., 2018; Karner et al., 2010; Liu et al., 2019), and light pollution from streetlights and from vehicle headlights (Gaston and Holt, 2018). In each case, we used the full text to extract the following information (where available) for each form of pollution: source strength $a$, background level $b$, decay rate $\lambda$ (or otherwise pollution level at multiple distances), and the relationship between pollution level and traffic volume. We used WebPlotDigitizer 4.2 (Rohatgi, 2015) to extract information from figures where necessary. Karner et al. (2010) provided regressions of pollution level over distance, rather than explicit decay rates, so we extracted the distance at which the pollution level had decayed by 90% from the source strength towards the background level, then used this to calculate an exponential decay rate. We used a level of 90% because we assumed that the underlying pollution measurement data has low power when it comes to detecting pollution levels that have more closely approached the background level (the tail of the exponential decay curve). Similarly, Werkenthin et al. (2014) only provided pollution levels for three distance categories (0–5, 5–10 and 10–25 m from roads), so we calculated a decay rate based on changes in the median pollution level across distance categories – resulting in either $\lambda = 0.2303$ or $\lambda = 0.0921$, reflecting 90% decay of pollution source strength towards the background level by 10 and 25 m, respectively.

### *2.4. Assumptions for missing parameter values*

Whilst the literature search provided sufficient parameter values for decay rates $\lambda$, information on source pollution strengths $a$ and relationships with traffic volume $x$ were mostly lacking. We therefore sought additional data and were required to make several assumptions (Table B). These are described below, with the final parameter values for each form of pollution presented in Table 2.

#### *2.4.1. Metals and air pollutants*

For pollution source strengths, we used UK government data for air pollutants ($NO_2$, $PM_{2.5}$, $PM_{10}$) from 2019 (Table 2; Defra, 2020), which were similar to the levels measured in the USA by DeWinter et al. (2018). For both air pollutants and metals, we assumed that median source strengths from the empirical data were representative of A-roads ($r = 2$). Source strengths for other road types were proportional to their traffic volume scaled with $x = 0.75$ in Eq. (1), rather than $x = 1$ (whereby a 10 times increase in traffic volume results in a 10 times increase in pollution source strength when $x = 1$, and in a 5.62 times increase in pollution source strength when $x = 0.75$), because we assumed that vehicles on smaller, lower traffic roads brake and accelerate more frequently, resulting in a proportionally greater amount of metals and air pollutants (Pandian et al., 2009). However, for $PM_{2.5}$ we used Eq. (1) with $x = 0.5$ (whereby a ten-fold increase in traffic volume results in a 3.16 times increase in pollution source strength) to reflect a weaker relationship between traffic volume and source pollution strength (DeWinter et al., 2018). Reviews of $NO_2$ dispersion provided dramatically different decay rates of $\lambda = 0.0064$ (Karner et al., 2010) and $\lambda = 0.0004$ (Liu et al., 2019), which is equivalent to a ten-fold difference in extent. This is apparently because Liu et al. (2019) did not account for background pollution levels. We therefore used the more conservative and relevant estimates from Karner et al. (2010). We note that air pollution dispersion patterns from the literature are primarily based on downwind measurements (Karner et al., 2010; Liu et al., 2019), whereas in reality dispersion patterns are asymmetrical due to wind direction, and predominant in one direction due to prevailing winds. For simplicity, we use downwind dispersion patterns in all directions, which indicates the maximum potential extent of air pollutants.

#### *2.4.2. Light and noise*

Light and noise arising from vehicles consist of both an intensity and a frequency component, which are both likely to be relevant in triggering ecological responses. We therefore considered both single event exposure level (i.e. when a vehicle passed), and average exposure level, which accounts for differences in traffic volume between road types.

Noise is commonly expressed in units of decibels – a logarithmic scale which is used as a more representative measure of the perception of changes in noise intensity by biological organisms. We therefore converted to and from source and estimated noise levels in terms of the log scale of decibels using the standard equation $dB = 10 \log p$, where $p$ is the sound power ratio, which is the unit that decays over distance following the inverse square law. We assumed that noise exposure source strength was 85 dB for all road types (Bendtsen, 1999). Whilst heavy vehicles and vehicles travelling at greater speeds produce more noise (Bendtsen, 1999), which are likely to be more common on motorways and A-roads, such noise levels probably often occur across all road types because component roads are highly heterogeneous, and speed limits are similar across road types (70 mph (113 km $h^{-1}$) for motorways, and most frequently 60 mph (97 km $h^{-1}$) for other road types because we didn't distinguish urban from rural roads). For average noise exposure level, we estimated source strengths for each road type using Eq. (1) with $a_1 = 85$ dB and $x = 1$. These assumptions result in average noise source strengths for each road type that are similar to those used in previous national-scale modelling of noise across Great Britain (Jackson et al., 2008).

**Table 2**
Summary of the model parameter values, including those informed by the literature search (λ, a and b), and those that were otherwise estimated (primarily x; see Methods). These parameters were used to produce Figs. 2–3. Full details, including assumptions and limitations of these synthesised parameters, are described in Table B.

| Form of road pollution | Units | Decay type | Source pollution level ~ traffic scaling factor ($x$) | Decay rate ($\lambda$) | Pollution source strength ($a$) | Background pollution level ($b$) | Data sources |
|---|---|---|---|---|---|---|---|
| Light pollution | | | | | | | |
| Streetlights | | | | | | | |
| Single event exposure | lx | Inverse square | n/a | n/a | 4800 | 0 | Gaston and Holt (2018) |
| Average exposure | | | (1,1,0,0 for $r = 1,2,3,4$) | n/a | 4800 | 0 | |
| Vehicle headlights | | | | | | | |
| Single event exposure | | | 0 | n/a | 9200 | 0 | |
| Average exposure | | | 1 | n/a | 9200 | 0 | |
| Noise pollution | | | | | | | |
| Single event exposure | dB | Inverse square | 0 | n/a | 85 | 0 | Attenborough (2014) |
| Average exposure | | | 1 | n/a | 85 | 0 | |
| Metal pollution | | | | | | | |
| Cadmium (Cd) | ppm | Exponential | 0.75 | 0.0921 | 0.73 | 0.21 | Werkenthin et al. (2014) |
| Chromium (Cr) | | | 0.75 | 0.2303 | 28.0 | 25.7 | |
| Copper (Cu) | | | 0.75 | 0.2303 | 47.9 | 13.6 | |
| Nickel (Ni) | | | 0.75 | 0.2303 | 24.5 | 20.2 | |
| Lead (Pb) | | | 0.75 | 0.0921 | 106.0 | 23.5 | |
| Zinc (Zn) | | | 0.75 | 0.2303 | 179.5 | 52.9 | |
| Air pollutants | | | | | | | |
| $NO_2$ | ppb | Exponential | 0.75 | 0.0064 | 31 | 7 | Defra (2020); |
| $PM_{2.5}$ | | | 0.5 | 0.0023 | 10.08 | 9.87 | DeWinter et al. (2018); |
| $PM_{10}$ | | | 0.75 | 0.0200 | 18 | 15 | Karner et al. (2010) |

Vehicle headlights produce a concentrated horizontal beam that attenuates at a lower rate than described by an inverse square decay, but this is generally directed largely parallel rather than perpendicular to a road so we also assumed that decay of this light perpendicular to the road follows an inverse square relationship. For light arising from streetlights, we assumed that streetlights are always turned on at night-time (so the single event exposure level, as used for noise and light from vehicle headlights, is equivalent to the average exposure level), and that they are found on all motorways and A-roads, but not on minor roads or local roads (Table 2). In reality, streetlights are often found along minor roads in urban areas, but these were not distinguished from rural roads in our road type groupings.

## 2.5. Spatial modelling

### 2.5.1. Real forms of road pollution

We modelled, in absolute terms, the spatial distributions of metals in soils (Cd, Cr, Cu, Ni, Pb, and Zn), of air pollutants ($NO_2$, and particulate matter $PM_{2.5}$ and $PM_{10}$) (particles), and of light and noise (energy waves) arising from roads. Modelling used Eqs. (1)–(7), combined with parameter values gathered from the literature search, and supplemented with the estimates and assumptions described above to provide missing values (Table 2).

We describe the spatial distribution of pollution consisting of matter using thresholds of 50%, 25%, 10%, 1%, and 0.1% of the source strength found along the busiest road type (motorways). Whilst 0.1% appears to be small, it is equivalent to elevated levels of 0.002 ppm Cd, 0.01 ppm Cr, 0.13 ppm Cu, 0.02 ppm Ni, 0.31 ppm Pb, 0.48 ppm Zn, 0.09 ppb $NO_2$, 0.0005 ppb $PM_{2.5}$, and 0.01 ppb $PM_{10}$ (Fig. 2). These metal concentrations are similar to the maximum guidelines for drinking water (World Health Organization, 2017) and, for example, such levels of lead have been found to have effects on animal physiology (Boskabady et al., 2018). Real measurements of pollution levels will generally be much greater because our models do not include background levels or pollution from non-road sources. For light and noise (energy waves), we use thresholds of 10%, 1%, 0.1%, 0.01%, and 0.001% of the source strength (Fig. 3) because a logarithmic scale is more representative of the perceived changes in these forms of pollution by organisms. For light 0.001% of the source strength is equivalent to elevated levels of 0.1 lx – comparable to full moonlight under a clear sky, which is known to have ecological impacts (Gaston et al., 2013; Sanders et al., 2020). For noise 0.001% is equivalent to 30 dB – above which effects on human sleep are observed (Basner and McGuire, 2018). Levels above 0.1% for matter, and above 0.001% for energy waves, are therefore described as elevated. This cut-off was necessary because exponential and inverse square decay functions have long tails that approach, but never reach, zero. For each pollutant, we calculated the proportion of raster cells above threshold pollution levels of interest, then converted this to an estimate of land area ($km^2$).

### 2.5.2. Theoretical road pollution groups

Given limitations on available data for different forms of road pollution, we modelled the spatial dispersion of theoretical pollution groups that varied in their pollution source strengths and dispersion patterns, across a range that encompasses those of real forms of road pollution.

We considered nine values of x (1.5, 1.25, 1, 0.75, 0.5 0.25, 0.1, 0.05, and 0) that covered the full realistic range of relationships between traffic volume and pollution source strength, from disproportionately large effects ($x > 1$), to simple additive effects ($x = 1$), to increasingly diminishing effects ($x < 1$), of increasing traffic volume (Table C). As the modelled pollution level was relative, rather than absolute, the background pollution level $b$ was not required. We considered values for decay rates λ that resulted in the pollution level decreasing by 90% of its source strength at distances of 10, 25, 50, 100, 250, 500, 1000, and 2500 m from the source, a total of eight different decay rates (Table C). We considered all combinations of pollution source strengths $a$ (values of $x$ in Eq. (1)), and decay rates λ for models of pollution types that consist of matter – a total of 81 pollution groups (Fig. A; Table C).

## 3. Results

### 3.1. Distance to nearest road

Using 100 m resolution maps to calculate the distance of each 100 m centroid to the nearest road, shows that 25% of land is less than 79 m from a road, 50% less than 216 m and 75% less than 527 m (Fig. 1). In most cases, the nearest road is a minor or local access road, as these constitute 49% and 43%, respectively, of total road length, compared to the 8% of total road length that comprises more major roads (motorways and A-roads; Table 1). Roadless areas (>1 km from roads) are scarce,

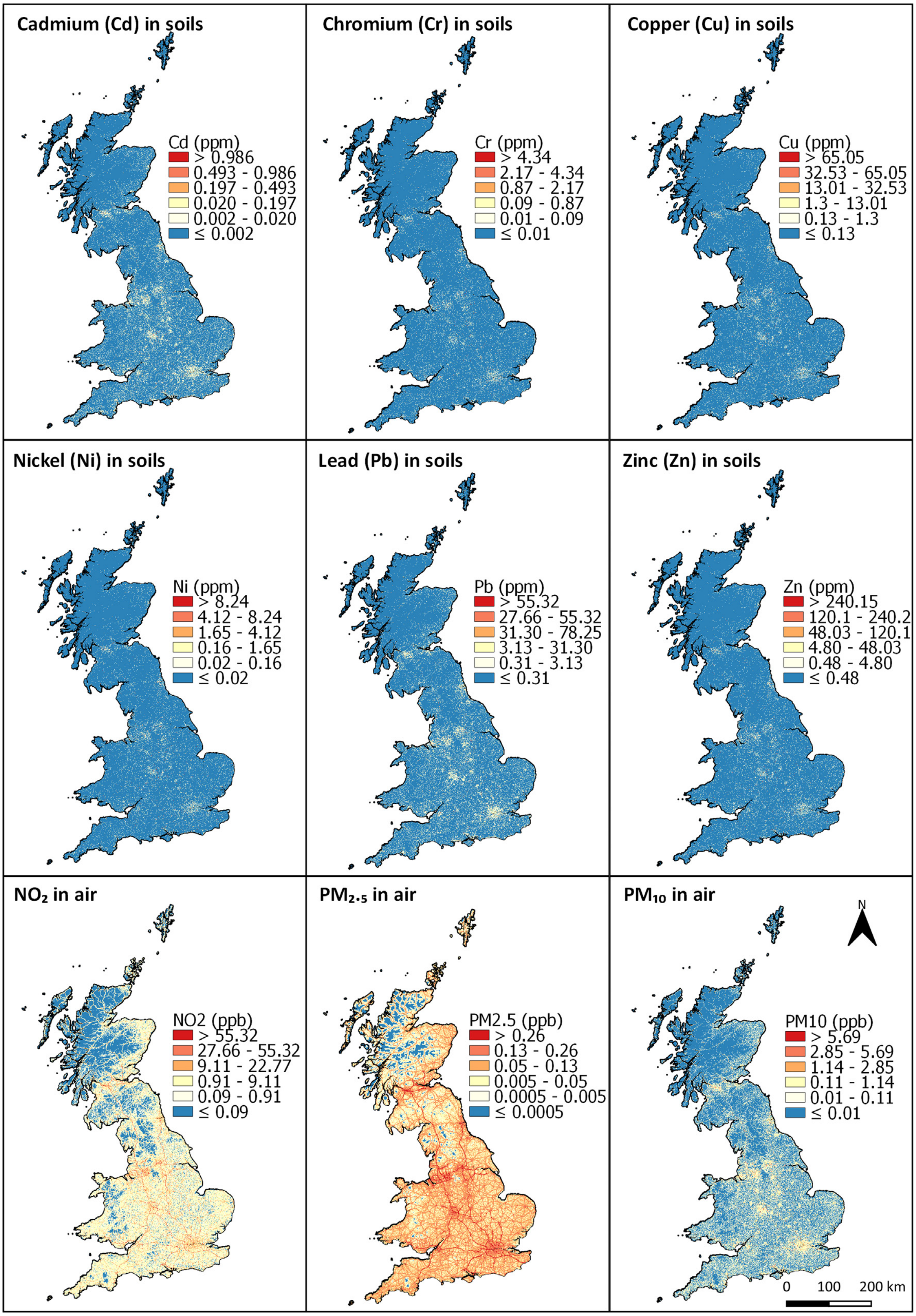


**Fig. 2.** The modelled spatial distributions of metals and air pollutants arising from roads across Great Britain. Values are pollution levels exclusively attributable to roads, i.e. additional pollution produced by roads beyond the background level, rather than the absolute pollution level (incorporating all sources). Maps were produced using Eqs. (1)–(7) and the parameter values in Table 2.

covering only 11.8% of land, and confined almost exclusively to the uplands (Fig. 1). Specifically, these areas have a mean elevation of 391 m (median = 386 m, $SD$ = 218 m), and are composed of the following land covers: 47% peat bogs, 23% moors and heathland, 14% natural grasslands, and 8% sparsely vegetated areas. Only 3.6% of land is more than 2.5 km from roads (Fig. 1). For comparison, based on a total length

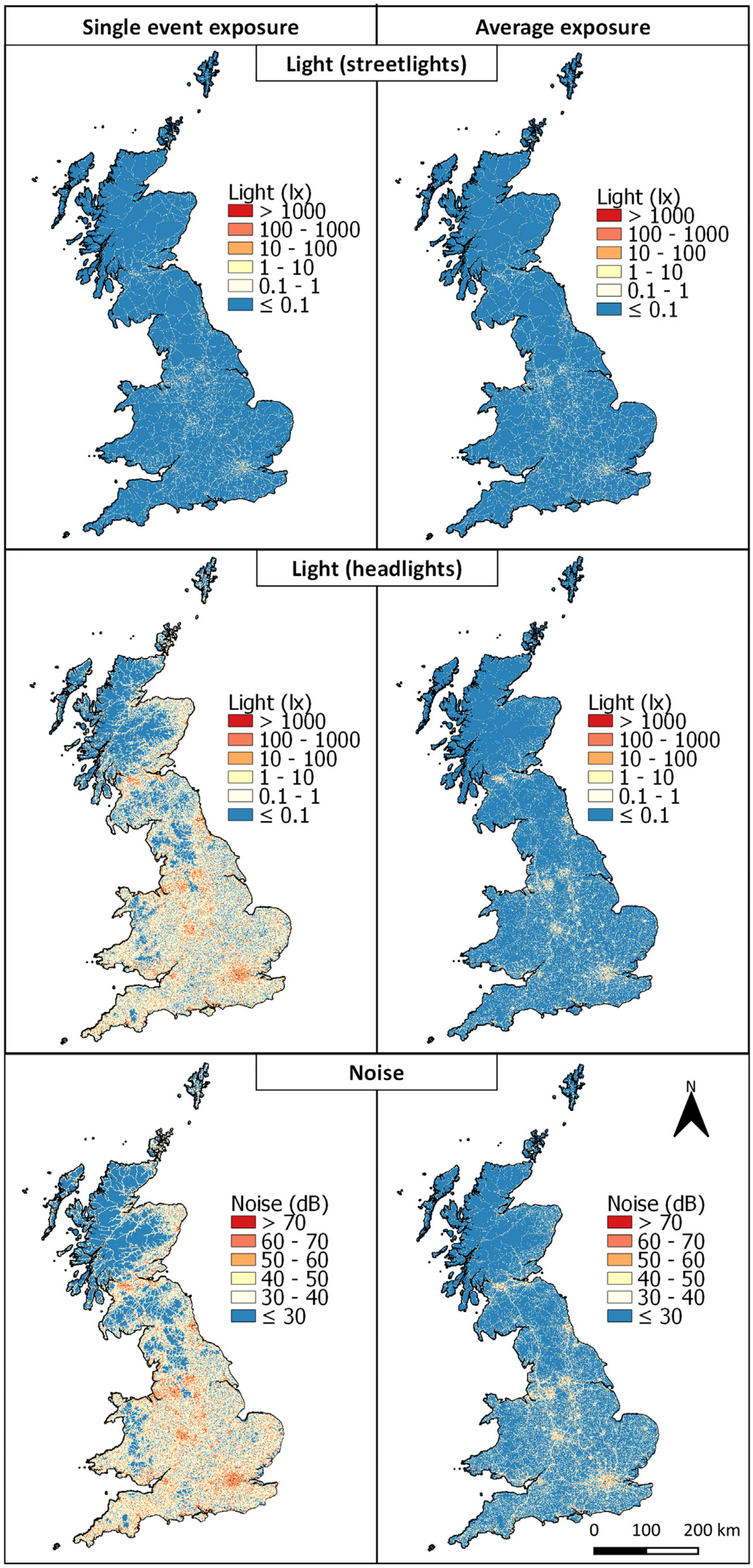


**Fig. 3.** The modelled spatial distributions of light and noise arising from roads across Great Britain. Values are pollution levels exclusively attributable to roads, i.e. additional pollution produced by roads beyond the background level, rather than the absolute pollution level (incorporating all sources). Single event exposure level represents the typical level experienced when a vehicle passes on the nearest road, whereas average exposure level accounts for differences in traffic volume between road types. Maps were produced using Eqs. (1)–(7) and the parameter values in Table 2.

**Table 3**
Estimated area of land in Great Britain affected by different forms of road pollution (from Figs. 2–3).

| Form of road pollution | Pollution level | Estimated area of land in Great Britain affected | |
|---|---|---|---|
| | | Area of land ($km^2$) | % of land |
| Light (streetlights) – single event exposure level | >1000 lx | 374 | 0.18 |
| | >100 lx | 1104 | 0.53 |
| | >10 lx | 2492 | 1.19 |
| | >1 lx | 6667 | 3.18 |
| | >0.1 lx | 19,109 | 9.13 |
| Light (streetlights) – average exposure level | >1000 lx | 374 | 0.18 |
| | >100 lx | 1104 | 0.53 |
| | >10 lx | 2492 | 1.19 |
| | >1 lx | 6667 | 3.18 |
| | >0.1 lx | 19,109 | 9.13 |
| Light (headlights) – single event exposure level | >1000 lx | 4300 | 2.05 |
| | >100 lx | 11,044 | 5.28 |
| | >10 lx | 29,567 | 14.12 |
| | >1 lx | 71,134 | 33.98 |
| | >0.1 lx | 147,220 | 70.33 |
| Light (headlights) – average exposure level | >1000 lx | 178 | 0.09 |
| | >100 lx | 1743 | 0.83 |
| | >10 lx | 4928 | 2.35 |
| | >1 lx | 13,683 | 6.54 |
| | >0.1 lx | 35,360 | 16.89 |
| Noise – single event exposure level | >70 dB | 5142 | 2.46 |
| | >60 dB | 13,316 | 6.36 |
| | >50 dB | 33,838 | 16.16 |
| | >40 dB | 77,124 | 36.84 |
| | >30 dB | 147,147 | 70.29 |
| Noise – average exposure level | >70 dB | 458 | 0.22 |
| | >60 dB | 3346 | 1.60 |
| | >50 dB | 8728 | 4.17 |
| | >40 dB | 23,133 | 11.05 |
| | >30 dB | 55,834 | 26.67 |
| Cadmium (Cd) in soils | >1 ppm | 138 | 0.07 |
| | >0.5 ppm | 644 | 0.31 |
| | >0.25 ppm | 1356 | 0.65 |
| | >0.025 ppm | 12,787 | 6.11 |
| | >0.0025 ppm | 30,363 | 14.50 |
| Chromium (Cr) in soils | >5.00 ppm | 202 | 0.10 |
| | >2.50 ppm | 489 | 0.23 |
| | >1.25 ppm | 777 | 0.37 |
| | >0.125 ppm | 5641 | 2.69 |
| | >0.0125 ppm | 13,977 | 6.68 |
| Copper (Cu) in soils | >60.00 ppm | 295 | 0.14 |
| | >30.00 ppm | 582 | 0.28 |
| | >15.00 ppm | 868 | 0.41 |
| | >1.50 ppm | 6300 | 3.01 |
| | >0.15 ppm | 14,838 | 7.09 |
| Nickel (Ni) in soils | >10.00 ppm | 180 | 0.09 |
| | >5.00 ppm | 467 | 0.22 |
| | >2.50 ppm | 756 | 0.36 |
| | >0.25 ppm | 5488 | 2.62 |
| | >0.025 ppm | 13,778 | 6.58 |
| Lead (Pb) in soils | >50.00 ppm | 1117 | 0.53 |
| | >25.00 ppm | 1833 | 0.88 |
| | >12.50 ppm | 4524 | 2.16 |
| | >1.25 ppm | 21,302 | 10.18 |
| | >0.125 ppm | 38,283 | 18.29 |
| Zinc (Zn) in soils | >250.00 ppm | 245 | 0.12 |
| | >125.00 ppm | 531 | 0.25 |
| | >62.50 ppm | 818 | 0.39 |
| | >6.25 ppm | 5942 | 2.84 |
| | >0.625 ppm | 14,368 | 6.86 |
| $NO_2$ in air | >50.00 ppb | 834 | 0.40 |
| | >25.00 ppb | 2762 | 1.32 |
| | >12.50 ppb | 13,104 | 6.26 |
| | >1.25 ppb | 94,973 | 45.37 |
| | >0.125 ppb | 157,290 | 75.14 |
| $PM_{2.5}$ in air | >0.2 ppb | 16,872 | 8.06 |
| | >0.1 ppb | 48,375 | 23.11 |
| | >0.05 ppb | 111,298 | 53.17 |
| | >0.005 ppb | 183,718 | 87.76 |
| | >0.0005 ppb | 197,691 | 94.44 |
| $PM_{10}$ in air | >5.00 ppb | 1837 | 0.88 |
| | >2.50 ppb | 352 | 0.17 |
| | >1.25 ppb | 4737 | 2.26 |
| | >0.125 ppb | 41,638 | 19.89 |
| | >0.0125 ppb | 83,493 | 39.89 |

of road of 690,680 km across Great Britain (including the 294,196 km of local access roads, which are generally not considered in national estimates of road length; Table 1), we estimate that roads cover 1934 $km^2$ (0.8% of land), with an average road density of 2.84 km of road/$km^2$ of land. This estimate includes the paved road surface, but not related hard and soft surfaces either side of, or in between, road lanes (e.g. pavements, laybys, central reservations, and road verges).

### 3.2. Spatial distribution of real forms of road pollution

Considering real forms of road pollution for which there were data to estimate their patterns of spread from roads, high levels (e.g. >10% of source strength) are relatively localised (Figs. 2–3). However, elevated levels occur across an estimated 94% of land in Great Britain, especially for $NO_2$, $PM_{2.5}$, noise and light (Figs. 2–3). Again, the only land to escape pollution from roads is located almost entirely in the uplands.

The proportion of land affected by 10% or more of the pollution levels found at the source along the busiest roads amounts to 9% for $NO_2$ and 52% for $PM_{2.5}$. The respective proportion of land affected by 1% or more of these pollutants is 51% for $NO_2$, 84% for $PM_{2.5}$, and by 0.1% or more is 77% and 94%. Based on estimated concentrations of these pollutants at roadsides, 45% of land is affected by $NO_2$ levels elevated by at least 1.25 ppb due to roads, and 88% of land in Great Britain is affected by $PM_{2.5}$ levels elevated by at least 0.005 ppb due to roads. Due to the pervasiveness of roads, and of light and noise arising from vehicles on them, most land is likely to be exposed to some pollution. For example, when vehicles pass by on nearby roads, an estimated 70% of land in Great Britain is exposed to elevated light pollution of at least 0.1 lx, and to elevated noise pollution of at least 30 dB (0.001% of the source strength found along the busiest road type – motorways). Taking account of the frequency of light and noise pollution due to intermittent traffic, 16% of land is affected by average light levels from roads of at least 0.1 lx, and 27% of land is affected by average noise levels from roads of above 30 dB (Fig. 3). Additional results are provided in Table 3.

### 3.3. Spatial distribution of theoretical road pollution groups

Given limitations on available data for the dispersion of different pollutants from roads, we generalised our findings by modelling the spatial dispersion of theoretical pollution groups with different characteristics. Again, this shows that high levels of road pollution (e.g. >10% source strength) are generally localised (Figs. 4–5). However, pollution need only extend 250 m or more from roads, even if highly concentrated around high traffic volume roads, for it to affect at least 50% of land in Great Britain at levels above 0.1% of those found alongside the busiest roads (Figs. 4–5). Overall, minor roads and local access roads have major potential to cause widespread pollution and environmental impacts due to their substantially greater extent than motorways and A-roads (Table 1). As the dispersal distance of a pollutant increases – from a 90% decay within 10 m to a 90% decay within 250 m – the total land area affected rapidly increases, regardless of whether pollution primarily arises from high traffic roads or more evenly across road types (Figs. 4–5). However, for forms of pollution arising primarily from high traffic volume roads, pollution is far more localised. Overall,

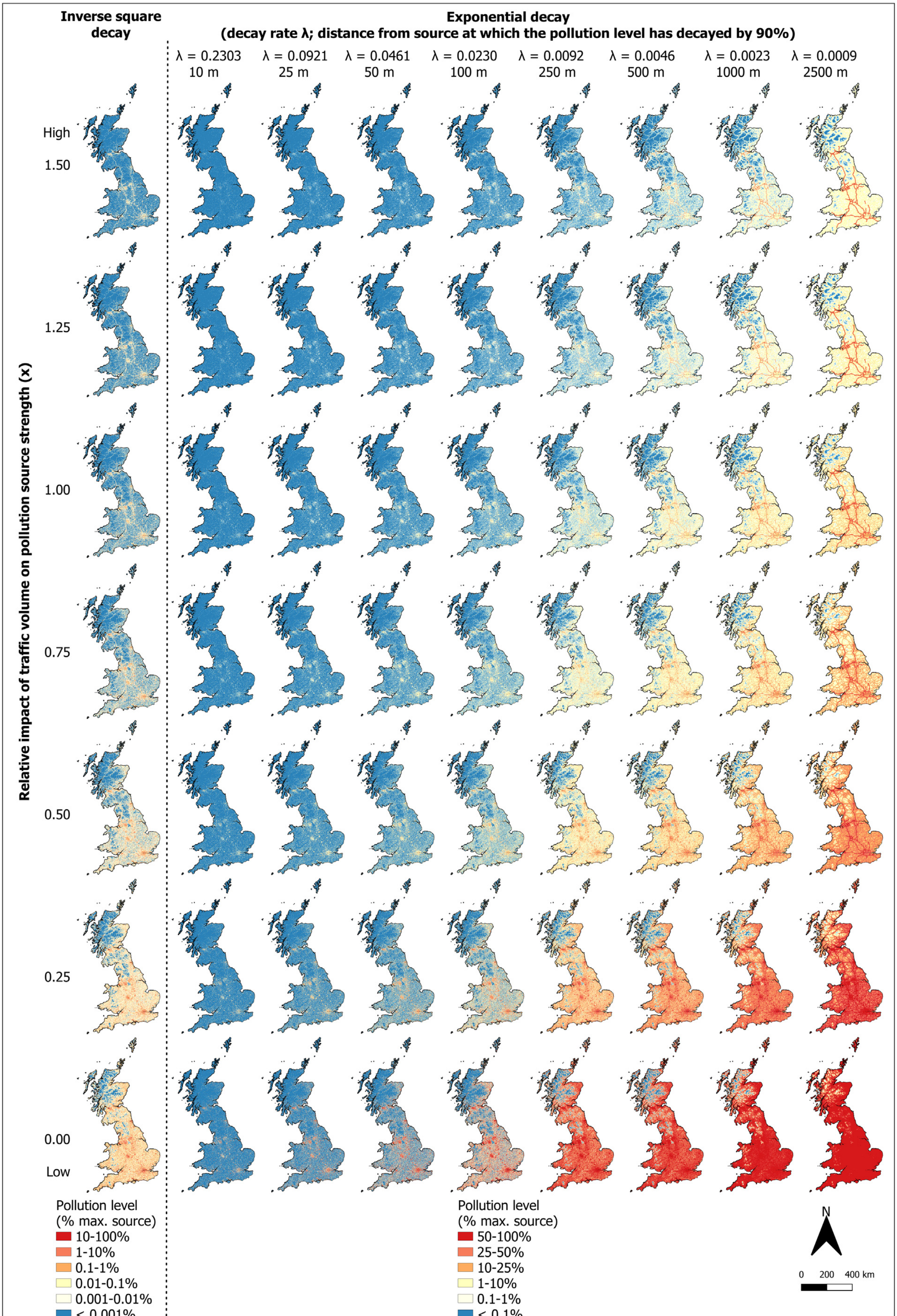
Inverse square decay
Exponential decay
(decay rate λ; distance from source at which the pollution level has decayed by 90%)
λ = 0.2303 10 m
λ = 0.0921 25 m
λ = 0.0461 50 m
λ = 0.0230 100 m
λ = 0.0092 250 m
λ = 0.0046 500 m
λ = 0.0023 1000 m
λ = 0.0009 2500 m
Relative impact of traffic volume on pollution source strength (x)
High
1.50
1.25
1.00
0.75
0.50
0.25
0.00
Low
Pollution level (% max. source)
10-100%
1-10%
0.1-1%
0.01-0.1%
0.001-0.01%
< 0.001%
Pollution level (% max. source)
50-100%
25-50%
10-25%
1-10%
0.1-1%
< 0.1%
N
0 200 400 km

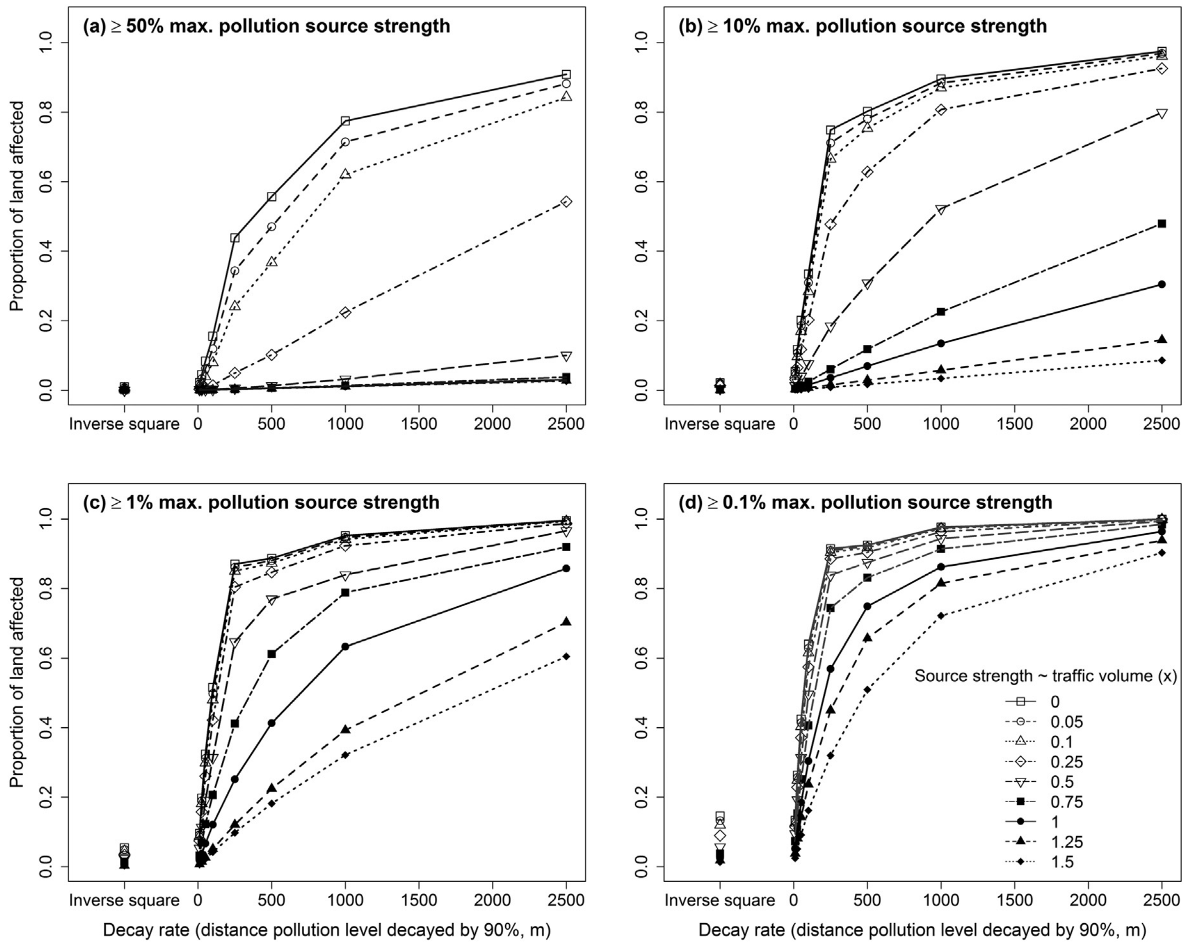


**Fig. 5.** The proportion of land in Great Britain affected by (a) ≥50%, (b) ≥10%, (c) ≥1% and (d) ≥0.1% of the maximum pollution source strength (i.e. that observed along motorways – the highest traffic volume road type), for each theoretical pollution group – varying in decay type: inverse square or exponential with varying decay rate, λ, and relative impact of traffic volume on pollution source strength ($x$), i.e. level of clustering of pollution around high traffic volume roads (see Eqs. (1)–(7) and Table C). These data summarise the patterns in Fig. 4.

theoretical forms of pollution with relatively rapid decay (that decay by 90% within 250 m), and arising primarily from high traffic roads, are present at high levels only over limited extents (i.e. <20% of land) (Fig. 5a–b). However, at low levels (>0.1% of source strength) that might still be environmentally relevant, they can extend across large areas (i.e. >50% of land) (Fig. 5c–d). For example, pollution that extends 100 m from roads is still likely to cover more than half of Great Britain, albeit at low levels (>0.1–1% of source strength), unless arising almost exclusively from high traffic roads (Fig. 5c–d).

## 4. Discussion

Using realistic estimates of how pollution levels decay with distance, our study suggests that, whilst the greatest levels of road pollution are relatively localised, low levels of road pollution are pervasive. Specifically, mapping of pollutants for which sufficient data are available shows that roads may have a zone of influence (road-effect zone) that extends across at least 70% of land in Great Britain, and potentially less than 6% of land escapes any impact. This is in strong contrast to the relatively small area of land that roads themselves cover (an estimated 0.8% of land). Previous studies have emphasised the importance of protecting roadless areas from further road building for nature conservation purposes (Ibisch et al., 2016; Psaralexi et al., 2017; Selva et al., 2011), and our study shows that the rarity of such areas in Great Britain makes them even more important. Yet, the limited extent of roadless areas, and the fact that they are located almost exclusively in the uplands, shows that protecting them has limited capacity to protect species and ecosystems that are vulnerable to road pollution, or people's health. Instead, it validates the rationale for our study to look at how road impacts vary within road-effect zones.

Our findings have important implications for research and policy. Namely, we suggest that the extent of roads' influence on the environment has been somewhat overlooked and underestimated. As with light pollution and the intensification of agriculture, environmental pressures from roads have largely arisen, and rapidly grown, over the past 50–100 years, and may now be so pervasive that their effects are difficult to distinguish and disentangle, and so are not fully appreciated. Our study justifies a major research effort to evaluate the extent, pathways and impacts of the many poorly studied forms of road pollution. Whilst research is lacking for most forms of pollution and their potential environmental impacts, studies of human health suggest that impacts on people occur across almost the entire range of most air pollutants

**Fig. 4.** The modelled spatial distribution of road pollution across Great Britain for the theoretical pollution groups that vary in decay type (inverse square or exponential with varying decay rate, λ) and relative impact of traffic volume on pollution source strength ($x$), i.e. level of clustering of pollution around high traffic volume roads (see Eqs. (1)–(7) and Table C). Note that inverse square decay (representing energy wave pollutants, e.g. light) uses a different scale to exponential decay (representing matter pollutants, e.g. gases) because a logarithmic scale is more representative of the perceived changes in energy wave pollutants by organisms (see Methods).

(e.g. up to 100–400 m from roads for particulate matter and 200–500 m for $NO_2$; Zhou and Levy, 2007), which can have similar respiratory and other impacts on birds (Sanderfoot and Holloway, 2017), mammals (Llacuna et al., 1996) and insects (Thimmegowda et al., 2020). Recent evidence suggests that road impacts can scale up to population-level effects for birds and mammals (Benítez-López et al., 2010; Cooke et al., 2020a, 2020b; Torres et al., 2016), with estimated effects up to distances of 1 km and 5 km, respectively, so affecting 55.5% and 97.9% of land across Europe (Benítez-López et al., 2010; Torres et al., 2016). However, little is known about if and how impacts on other taxa scale up, or about how different impacts interact. In summary, the ubiquity of road pollution should be seriously considered as a potential contributor to global- and regional-scale environmental issues such as insect declines (Wagner, 2020) and microplastic pollution (Evangeliou et al., 2020).

Looking at effects as they attenuate with distance from roads is more realistic than assuming a simple cut off with distance, as has previously been used (Ibisch et al., 2016; Psaralexi et al., 2017). Whilst a rule of thumb can be assumed whereby further from roads is better, our study shows that a mechanistic approach is much more appropriate because impacts also depend on the type of road, type of pollution and threshold for environmental impacts. A major advantage of our study is that we have considered the diverse forms of pollution from roads at large scales. However, we were required by necessity to make assumptions and simplifications. We can infer that our relatively simple models estimate maximum potential extent because we largely ignore mitigation by vegetation, terrain and other barriers. In reality there is likely to be much greater spatial and temporal clustering of pollutants and road impacts, for example due to additive effects of multiple nearby roads of the same type, heterogeneity of traffic volumes between roads and across time, and local factors such as tall buildings in urban areas forming street canyons that can trap and thus concentrate air pollutants (Vardoulakis et al., 2007). However, it should be noted that our study did not include the influence of streams and rivers in transporting pollutants, or the marine area affected by road pollution, which would have increased the estimated extent, possibly substantially so if atmospheric and oceanic currents were accounted for (Evangeliou et al., 2020).

Whilst decay rates are available for many pollutants, our study highlights a lack of data on how source pollution strengths vary across road types, or of the environmental impacts of lower levels of road pollution. In this case, we estimated a number of parameter values for road pollutants (Table 2), then looked across the full range of values (Fig. 4) to show how changes in these values would affect the spatial distributions of these forms of pollution. However, future research should aim to fill these data gaps. Most studies have unsurprisingly focused on the largest, busiest roads, and on the high levels of pollution found in their immediate or near vicinity. However, to comprehend the scale of roads influence on the environment, it is essential to understand the impacts of pervasive, low levels of pollution. Improvements in sensing technologies (e.g. Asdrubali and D'Alessandro, 2018) will increasingly make more widespread monitoring of road pollution possible.

Whilst we used Great Britain as a study area, the findings likely apply to other densely populated regions at present, and to many additional regions in the future due to the predicted rapid expansion of the global road network. Great Britain has road densities towards the upper limit of those found worldwide – an estimated 2.84 km of road/km$^2$ of land. Whilst we found that distances to roads were somewhat greater than averages reported for the USA (Riitters and Wickham, 2003), for Europe as a whole (Psaralexi et al., 2017; Torres et al., 2016), and worldwide (Ibisch et al., 2016), differences partly reflect the more complete underlying road maps used in our work compared to in previous studies (Hughes, 2017), which included local access roads and other low traffic roads. In reality, many regions of Europe and North America likely have similarly high densities of roads (Ibisch et al., 2016; Psaralexi et al., 2017) and such densities will increasingly become the norm given a forecast 60% growth in the global road network by 2050 (Dulac, 2013). In fact, relatively greater environmental regulation of vehicle pollution in the UK likely means that environmental impacts per road vehicle are less than in many other regions. Given rapid expansion in road networks, and changes in road-use and vehicle technologies over the coming decades, there is an urgent need for the environmental influence of roads to become a more major focus of both research and policy.

Supplementary data to this article can be found online at https://doi.org/10.1016/j.scitotenv.2021.145589.

## CRediT authorship contribution statement

**Benjamin B. Phillips**: Conceptualization, Methodology, Investigation, Writing – original draft, Writing – review & editing. **James M. Bullock**: Conceptualization, Methodology, Writing – review & editing, Supervision. **Juliet** L. **Osborne**: Conceptualization, Methodology, Writing – review & editing, Supervision. **Kevin J. Gaston**: Conceptualization, Methodology, Writing – review & editing, Supervision.

## Declaration of competing interest

The authors declare no competing interests.

## Acknowledgements

BBP was funded by a NERC GW4+ Doctoral Training Partnership (DTP) studentship from the Natural Environment Research Council (NERC) [NE/L002434/1], with additional funding from the Cornwall Area of Outstanding Natural Beauty unit.

## Data availability statement

All data supporting the results are provided in the manuscript and appendices, and were gathered or derived from the associated references.

## References

Asdrubali, F., D'Alessandro, F., 2018. Innovative approaches for noise management in smart cities: a review. Curr. Pollut. Reports 4, 143–153. https://doi.org/10.1007/s40726-018-0090-z.

Attenborough, K., 2014. Sound propagation in the atmosphere. Springer Handbook of Acoustics https://doi.org/10.1007/978-1-4939-0755-7.

Basner, M., McGuire, S., 2018. WHO environmental noise guidelines for the european region: a systematic review on environmental noise and effects on sleep. Int. J. Environ. Res. Public Health 15, 519. https://doi.org/10.3390/ijerph15030519.

Bendtsen, H., 1999. The Nordic prediction method for road traffic noise. Sci. Total Environ. 235, 331–338. https://doi.org/10.1016/S0048-9697(99)00216-8.

Benítez-López, A., Alkemade, R., Verweij, P.A., 2010. The impacts of roads and other infrastructure on mammal and bird populations: a meta-analysis. Biol. Conserv. 143, 1307–1316. https://doi.org/10.1016/j.biocon.2010.02.009.

Boskabady, M., Marefati, N., Farkhondeh, T., Shakeri, F., Farshbaf, A., Boskabady, M.H., 2018. The effect of environmental lead exposure on human health and the contribution of inflammatory mechanisms, a review. Environ. Int. 120, 404–420. https://doi.org/10.1016/j.envint.2018.08.013.

Cooke, S.C., Balmford, A., Donald, P.F., Newson, S.E., Johnston, A., 2020a. Roads as a contributor to landscape-scale variation in bird communities. Nat. Commun. 11, 1–10. https://doi.org/10.1038/s41467-020-16899-x.

Cooke, S.C., Balmford, A., Newson, S.E., Donald, P.F., 2020b. Variation in abundances of common bird species associated with roads. J. Appl. Ecol. 1–12. https://doi.org/10.1111/1365-2664.13614.

Copernicus, 2018. CORINE land cover - CLC 2018 [WWW Document]. URL. https://land.copernicus.eu/pan-european/corine-land-cover.

Defra, 2020. ENV02 - air quality statistics [WWW Document]. URL. https://www.gov.uk/government/statistical-data-sets/env02-air-quality-statistics.

Department for Transport, 2019. Road traffic statistics (TRA) statistical data set [WWW Document]. URL. https://www.gov.uk/government/statistical-data-sets/road-traffic-statistics-tra.

Department for Transport, 2020. Road lengths statistics (RDL) [WWW Document]. URL. https://www.gov.uk/government/statistical-data-sets/road-length-statistics-rdl.

Department for Transport, 2020a. Design Manual for Roads and Bridges (DMRB).

DeWinter, J.L., Brown, S.G., Seagram, A.F., Landsberg, K., Eisinger, D.S., 2018. A national-scale review of air pollutant concentrations measured in the U.S. near-road monitoring network during 2014 and 2015. Atmos. Environ. 183, 94–105. https://doi.org/10.1016/j.atmosenv.2018.04.003.

Dulac, J., 2013. Global land transport infrastructure requirements: estimating road and railway infrastructure capacity and costs to 2050 [WWW Document]. URL. https://webstore.iea.org/global-land-transport-infrastructure-requirements.
European Commission, 2021a. Air quality standards [WWW Document]. URL. https://ec.europa.eu/environment/air/quality/standards.htm.
European Commission, 2021b. Air pollution from the main sources - air emissions from road vehicles [WWW Document]. URL. https://ec.europa.eu/environment/air/sources/road.htm.
Evangeliou, N., Grythe, H., Klimont, Z., Heyes, C., Eckhardt, S., Lopez-Aparicio, S., Stohl, A., 2020. Atmospheric transport is a major pathway of microplastics to remote regions. Nat. Commun. 11, 3381. https://doi.org/10.1038/s41467-020-17201-9.
Extrium, 2020. Extrium noise and air quality viewer [WWW Document]. URL. http://www.extrium.co.uk/noiseviewer.html.
Forehead, H., Huynh, N., 2018. Review of modelling air pollution from traffic at street-level - the state of the science. Environ. Pollut. 241, 775–786. https://doi.org/10.1016/j.envpol.2018.06.019.
Forman, R.T.T., 2000. Estimate of the area affected ecologically by the road system in the United States. Conserv. Biol. 14, 31–35.
Forman, R.T.T., Sperling, D., Bissonette, J.A., Clevenger, A.P., Cutshall, C.D., Dale, V.H., Fahrig, L., France, R.L., Goldman, C.R., Heanue, K., Jones, J., Swanson, F., Turrentine, T., Winter, T.C., 2003. Road Ecology. Island Press.
Gaston, K.J., Holt, L.A., 2018. Nature, extent and ecological implications of night-time light from road vehicles. J. Appl. Ecol. 55, 2296–2307. https://doi.org/10.1111/1365-2664.13157.
Gaston, K.J., Bennie, J., Davies, T.W., Hopkins, J., 2013. The ecological impacts of nighttime light pollution: a mechanistic appraisal. Biol. Rev. 88, 912–927. https://doi.org/10.1111/brv.12036.
Hänninen, O., Knol, A.B., Jantunen, M., Lim, T.A., Conrad, A., Rappolder, M., Carrer, P., Fanetti, A.C., Kim, R., Buekers, J., Torfs, R., Iavarone, I., Classen, T., Hornberg, C., Mekel, O.C.L., 2014. Environmental burden of disease in Europe: assessing nine risk factors in six countries. Environ. Health Perspect. 122, 439–446. https://doi.org/10.1289/ehp.1206154.
Hughes, A.C., 2017. Global roadless areas: hidden roads. Science 355, 1381. https://doi.org/10.1126/science.aam6995.
Ibisch, P.L., Hoffmann, M.T., Kreft, S., Pe, G., Kati, V., Biber-freudenberger, L., Dellasala, D.A., Vale, M.M., Hobson, P.R., Selva, N., 2016. A global map of roadless areas and their conservation status. Science 354, 1423–1427. https://doi.org/10.1126/science.aaf7166.
Jackson, S., Fuller, D., Dunsford, H., Mowbray, R., Hext, S., MacFarlane, R., Haggett, C., 2008. Tranquillity mapping: developing a robust methodology for planning support. Report to the Campaign to Protect Rural England, Centre for Environmental & Spatial Analysis. Northumbria University, Bluespace Environments and the University of Newcastle Upon on Tyne.
Karner, A.A., Eisinger, D.S., Niemeier, D.A., 2010. Near-roadway air quality: synthesizing the findings from real-world data. Environ. Sci. Technol. 44, 5334–5344. https://doi.org/10.1021/es100008x.
Khan, J., Ketzel, M., Kakosimos, K., Sørensen, M., Jensen, S.S., 2018. Road traffic air and noise pollution exposure assessment – a review of tools and techniques. Sci. Total Environ. 634, 661–676. https://doi.org/10.1016/j.scitotenv.2018.03.374.
Laurance, W.F., Clements, G.R., Sloan, S., O'Connell, C.S., Mueller, N.D., Goosem, M., Venter, O., Edwards, D.P., Phalan, B., Balmford, A., Van Der Ree, R., Arrea, I.B., 2014. A global strategy for road building. Nature 513, 229–232. https://doi.org/10.1038/nature13717.
Liu, S.V., Chen, F. Lin, Xue, J., 2019. A meta-analysis of selected near-road air pollutants based on concentration decay rates. Heliyon 5, e02236. https://doi.org/10.1016/j.heliyon.2019.e02236.
Llacuna, S., Gorriz, A., Riera, M., Nadal, J., 1996. Effects of air pollution on hematological parameters in passerine birds and small mammals. Arch. Environ. Contam. Toxicol. 31, 148–152. https://doi.org/10.1007/BF00203919.
Murphy, E., Faulkner, J.P., Douglas, O., 2020. Current state-of-the-art and new directions in strategic environmental noise mapping. Curr. Pollut. Reports 6, 54–64. https://doi.org/10.1007/s40726-020-00141-9.
Ordnance Survey, 2020. OS OpenData [WWW Document]. URL. https://www.ordnancesurvey.co.uk/opendatadownload/products.html.
Pandian, S., Gokhale, S., Ghoshal, A.K., 2009. Evaluating effects of traffic and vehicle characteristics on vehicular emissions near traffic intersections. Transp. Res. Part D Transp. Environ. 14, 180–196. https://doi.org/10.1016/j.trd.2008.12.001.
Pinto, J.A., Kumar, P., Alonso, M.F., Andreão, W.L., Pedruzzi, R., dos Santos, F.S., Moreira, D.M., Albuquerque, T.T. de A., 2020. Traffic data in air quality modeling: a review of key variables, improvements in results, open problems and challenges in current research. Atmos. Pollut. Res. 11, 454–468. https://doi.org/10.1016/j.apr.2019.11.018.
Psaralexi, M.K., Votsi, N.E.P., Selva, N., Mazaris, A.D., Pantis, J.D., 2017. Importance of roadless areas for the European conservation network. Front. Ecol. Evol. 5, 1–8. https://doi.org/10.3389/fevo.2017.00002.
QGIS Development Team, 2020. QGIS Geographic Information System.
van der Ree, R., Smith, D.J., Grilo, C., 2015. Handbook of Road Ecology. Wiley Blackwell, Oxford https://doi.org/10.1002/9781118568170.
Riitters, K.H., Wickham, J.D., 2003. How far to the nearest road? Front. Ecol. Environ. 1, 125–129. https://doi.org/10.1890/1540-9295(2003)001[0125:HFTTNR]2.0.CO;2.
Rohatgi, A., 2015. WebPlotDigitizer [WWW Document]. URL. https://automeris.io/WebPlotDigitizer.
Sanderfoot, O.V., Holloway, T., 2017. Air pollution impacts on avian species via inhalation exposure and associated outcomes. Environ. Res. Lett. 12. https://doi.org/10.1088/1748-9326/aa8051.
Sanders, D., Rago, E., Kehoe, R., Patterson, C., Gaston, K., 2020. A meta-analysis of biological impacts of artificial light at night. Nat. Ecol. Evol. https://doi.org/10.1038/s41559-020-01322-x.
Selva, N., Kreft, S., Kati, V., Schluck, M., Jonsson, B.G., Mihok, B., Okarma, H., Ibisch, P.L., 2011. Roadless and low-traffic areas as conservation targets in Europe. Environ. Manag. 48, 865–877. https://doi.org/10.1007/s00267-011-9751-z.
Silveira, C., Ferreira, J., Miranda, A.I., 2019. The challenges of air quality modelling when crossing multiple spatial scales. Air Qual. Atmos. Health 12, 1003–1017. https://doi.org/10.1007/s11869-019-00733-5.
Thimmegowda, G.G., Mullen, S., Sottilare, K., Sharma, A., Mohanta, S.S., Brockmann, A., Dhandapany, P.S., Olsson, S.B., 2020. A field-based quantitative analysis of sublethal effects of air pollution on pollinators. Proc. Natl. Acad. Sci. 117, 202009074. https://doi.org/10.1073/pnas.2009074117.
Torres, A., Jaeger, J.A.G., Alonso, J.C., 2016. Assessing large-scale wildlife responses to human infrastructure development. Proc. Natl. Acad. Sci. U. S. A. 113, 8472–8477. https://doi.org/10.1073/pnas.1522488113.
Tsagatakis, I., Ruddy, M., Richardson, J., Otto, A., Pearson, B., Passant, N., 2019. National Atmospheric Emissions Inventory - UK emission interactive map [WWW Document]. URL. https://naei.beis.gov.uk/emissionsapp/.
UK Government, 2021. Noise from roads, trains or planes [WWW Document]. URL. https://www.gov.uk/noise-pollution-road-train-plane/noise-from-roads.
Vardoulakis, S., Valiantis, M., Milner, J., ApSimon, H., 2007. Operational air pollution modelling in the UK-street canyon applications and challenges. Atmos. Environ. 41, 4622–4637. https://doi.org/10.1016/j.atmosenv.2007.03.039.
Wagner, D.L., 2020. Insect declines in the anthropocene. Annu. Rev. Entomol. 65, 457–480. https://doi.org/10.1146/annurev-ento-011019-025151.
Werkenthin, M., Kluge, B., Wessolek, G., 2014. Metals in European roadside soils and soil solution - a review. Environ. Pollut. 189, 98–110. https://doi.org/10.1016/j.envpol.2014.02.025.
World Health Organization, 2011. Burden of disease from environmental noise [WWW Document]. URL. https://www.who.int/quantifying_ehimpacts/publications/e94888.pdf.
World Health Organization, 2017. Guidelines for drinking-water quality [WWW Document]. URL. https://www.who.int/publications/i/item/9789241549950.
World Health Organization, 2018. Environmental noise guidelines for the European Region [WWW Document]. URL. https://www.euro.who.int/__data/assets/pdf_file/0008/383921/noise-guidelines-eng.pdf.
Zhou, Y., Levy, J.I., 2007. Factors influencing the spatial extent of mobile source air pollution impacts: a meta-analysis. BMC Public Health 7, 1–11. https://doi.org/10.1186/1471-2458-7-89.